

Slicing the Embryonic Chicken Auditory Brainstem to Evaluate Tonotopic Gradients and Microcircuits

Sandesh Mohan¹, Abhijit Roy¹, George Ordiway¹, Jason Tait Sanchez^{1,2,3}

¹ Roxelyn and Richard Department of Communication Sciences and Disorders, Northwestern University ² Knowles Hearing Research Center, Northwestern University ³ Department of Neurobiology, Northwestern University

Corresponding Author

Sandesh Mohan

sandesh.mohan@northwestern.edu

Citation

Mohan, S., Roy, A., Ordiway, G., Sanchez, J.T. Slicing the Embryonic Chicken Auditory Brainstem to Evaluate Tonotopic Gradients and Microcircuits. *J. Vis. Exp.* (185), e63476, doi:10.3791/63476 (2022).

Date Published

July 12, 2022

DOI

10.3791/63476

URL

jove.com/video/63476

Abstract

The chicken embryo is a widely accepted animal model to study the auditory brainstem, composed of highly specialized microcircuitry and neuronal topology differentially oriented along a tonotopic (i.e., frequency) axis. The tonotopic axis permits the segregated encoding of high-frequency sounds in the rostral-medial plane and low-frequency encoding in caudo-lateral regions. Traditionally, coronal brainstem slices of embryonic tissue permit the study of relative individual iso-frequency lamina. Although sufficient to investigate anatomical and physiological questions pertaining to individual iso-frequency regions, the study of tonotopic variation and its development across larger auditory brainstem areas is somewhat limited. This protocol reports brainstem slicing techniques from chicken embryos that encompass larger gradients of frequency regions in the lower auditory brainstem. The utilization of different slicing methods for chicken auditory brainstem tissue permits electrophysiological and anatomical experiments within one brainstem slice, where larger gradients of tonotopic properties and developmental trajectories are better preserved than coronal sections. Multiple slicing techniques allow for improved investigation of the diverse anatomical, biophysical, and tonotopic properties of auditory brainstem microcircuits.

Introduction

The chicken embryo is a valuable research model to study basic biological questions in numerous and diverse scientific areas including cell biology, immunology, pathology, and developmental neurobiology. The microcircuitry of the chicken auditory brainstem is an excellent example of a highly specialized circuit that can be understood in terms of auditory morphology and physiology. For example,

Rubel and Parks (1975) first described the tonotopic orientation (i.e., frequency gradient) of the chicken nucleus magnocellularis (NM) and nucleus laminaris (NL) as a linear function across the axis of the nuclei, oriented $\sim 30^\circ$ with respect to the sagittal plane. Individual neurons in NM and NL encode their best sound frequency-known as their characteristic frequency (CF)-along the rostral-medial plane

to the caudo-lateral region. High-frequency-sensitive neurons are in the rostral-medial region and low-frequency-sensitive neurons are located caudo-laterally. As such, traditional dissection methods of auditory brainstem tissue to study tonotopic properties have utilized successive coronal slices. Indeed, auditory microcircuits of developing chicken embryos have been established as a model system for studying signal processing of tonotopic auditory functions through successive caudal-to-rostral coronal plane brainstem slices for decades^{1,2,3,4,5,6}.

However, the tonotopic organization of NM and NL is topologically and morphologically convoluted. Auditory nerve inputs are distributed such that high CF inputs terminate in endbulb-like structures that cover at least one-quarter of an adendritic NM cell's somatic circumference. Conversely, low CF inputs are not organized with end bulb-like terminals but with multiple bouton synapses on dendrites of NM neurons. Middle CF inputs terminate as both end bulb and bouton-like synapses^{4,7,8,9,10,11,12}. In NL, the highly stereotyped dendritic gradient is evident not only in dendritic length but also in dendritic width. This unique dendritic gradient closely conforms to the tonotopic axis. The dendrites undergo an 11-fold increase in length and fivefold increase in width from high- to low-CF neurons, respectively⁶. To overcome such convoluted distributions of these nuclei in coronal slices, this protocol describes dissection approaches in the sagittal, horizontal, and horizontal/transverse planes. These slicing techniques provide examples of auditory brainstem tissue that exhibit maximum tonotopic properties in an individual slice plane.

Protocol

All procedures were approved by Northwestern University Institutional Animal Care and Use Committees (IACUC)

and were carried out in accordance with the National Institutes of Health Guidelines for the Care and Use of Laboratory Animals. The protocols for dissection and preparation of brainstem tissue are in adherence with previous protocols^{5,13}.

1. Egg handling

1. Purchase fertilized eggs (*Gallus gallus domesticus*) from an IACUC-approved local animal supplier.
2. Store the eggs immediately upon arrival in a refrigerator at 14 °C and incubate within 5 days.
NOTE: Embryo viability decreases considerably after 1 week.
3. Sterilize the eggs with 70% ethanol before incubation at 38 ± 1 °C and ~50% humidity.

2. Artificial cerebral-spinal fluid (ACSF) composition and preparation

1. Mix the following chemicals in 1 L of 18.2 MΩcm dH₂O to create a 10x ACSF stock solution: NaCl (sodium chloride) 130 mM, NaHCO₃ (sodium bicarbonate) 26 mM, KCl (potassium chloride) 2.5 mM, NaH₂PO₄ (sodium dihydrogen phosphate) 1.25 mM, dextrose (D-(+)-glucose) 10 mM. Keep the stock solution in the refrigerator.
2. Prepare MgCl₂ (magnesium chloride) 1 M and CaCl₂ (calcium chloride) 1 M solutions separately in 18.2 MΩcm dH₂O and store in the refrigerator.
3. Immediately before use, dilute 10x ACSF to 1x and bubble continuously with 95% O₂/5% CO₂ for 15-20 min and add MgCl₂ and CaCl₂. To prepare ACSF and dACSF (dissecting ACSF), adjust to a final concentration

of Mg^{2+} 1 mM, Ca^{2+} 3 mM and Mg^{2+} 3 mM, Ca^{2+} 1 mM, respectively.

4. Set the bubbling rate for the ACSF so that the pH is 7.2-7.4 with an osmolality between 300 and 310 mOsm/L.

NOTE: Having the ACSF placed in an ice bath while bubbling is beneficial for maintaining a low solution temperature, which will support tissue structural integrity while dissecting.

3. Agarose (5%) block preparation

1. Mix 5 g of agarose in 100 mL of dACSF. Use a 100 °C water bath or microwave for 2-3 min, stirring every 30 s to prevent lumps until the agarose dissolves completely and starts bubbling.
2. Pour the melted agarose in an empty Petri dish up to 5 mm thickness and keep at room temperature to set. After setting, seal the Petri dish using parafilm and store at 4 °C.
3. Cut the agarose into cubical blocks with a sharp blade and use them at the time of dissection.

4. Dissection protocol and isolating auditory brainstem

1. Clean the dissection area using 70% ethyl alcohol solution spray.
2. Glue the supporting or angled agarose block onto the vibratome tray.
3. Choose eggs of the desired age (E20 and E21 in the present protocol). Handle and incubate the eggs following the protocols listed above as in step 1.

4. Locate the air-filled space by placing the egg under a bright light (candling) and looking for this space on the larger or rounder side of the egg.
5. Acclimate the eggs to room temperature, crack the shell over the air-filled space, and expose the membrane sac.
6. Make a gentle incision in the sac to expose the beak.
7. With a scalpel, gently pull the neck and head out of the egg.
8. Quickly decapitate the head using sharp scissors.
9. After decapitation, clean the head with ice-chilled dACSF to remove excess blood from the dissection pad.
10. Hold the head steady in ice-chilled dACSF and make a rostro-caudal incision. Start the incision behind and between the eyes and follow the length of the harvested neck.

NOTE: Younger embryos may require less pressure while making the incision.
11. Separate the skin to expose the skull.
12. Cut the skull behind the eye in a midline to lateral direction. Do this for both hemispheres.

NOTE: This step helps separate the rostral portion of the skull from the attached brain while keeping the brain tissue intact⁵.
13. Slice the rostral portion of the skull. Place the blade behind the eyes and make a quick cut.

NOTE: Effort may be required to cut the attached skull cleanly.
14. Immerse the head in a dish of cold dACSF.
15. Utilizing a small pair of scissors, make midline to lateral incisions in the caudal region of the skull to try and

separate the brain from the skull without causing tissue damage.

16. Gently expose the brainstem and cerebellum. Retract the dorsal area of the entire skull, remove the brainstem carefully, and expose it with the help of a fine paintbrush with mild sledging. Use curved forceps to clean the brainstem from connecting tissue and blood vessels. Pay extra attention to the 8th cranial nerve area and be sure to leave a short length of intact nerve fibers on both sides.
17. Separate the brainstem from the cerebellum by cutting the peduncles and removing the blood vessels carefully. Trim the brainstem of additional blood vessels.

NOTE: Ensure that the whole procedure is performed in ice-chilled dACSF continuously bubbled with carboxygen (95% O₂/5% CO₂).

5. Vibratome slicing

NOTE: In the following steps, the back of the tissue must be supported with a cubical piece of agarose.

1. Place the vibratome blade along the horizontal axis and glue the brainstem on a slicing tray. Glue the rostral side, keeping the rostral-caudal axis vertical for coronal slices.
 1. Keep the lateral-medial axis vertical for sagittal slices.
 2. Glue the ventral side, keeping the dorsal-ventral axis vertical for horizontal slices.
2. To achieve the acute angular sagittal-horizontal plane, glue the brainstem's ventral side, keeping the ventral-dorsal axis vertical on the agarose block's hypotenuse surface, which is cut at a 45° angle. Glue the opposite surface of the agarose block facing the slicing tray and keep the rostral-caudal axis parallel to the blade edge.

6. Handling fragile or large pieces of brainstem tissue

1. In an alternative approach to step 5, immerse the isolated brainstem in 4% low melting point (LMP) agarose at ~40 °C in a 35 mm x 10 mm Petri dish.
 1. After pouring agarose on the immersed brainstem, place the Petri dish on ice to solidify. Cut the cubical agarose block with embedded brainstem using a sharp razor blade.
 2. Glue the LMP agarose block on its rostral side, keeping the brainstem's rostral-caudal axis vertical.
 1. Take coronal slices until the NM region can be visualized.
 2. Remove the agarose block from the glue with a sharp blade. To spot the nuclei, gently place 0.5 µL of dye (toluidine blue or orange G) on the NM with a fine needle.
 3. Remount this block on the slicing tray for sagittal or horizontal slices and identify the nuclei with respect to the stained region.
3. For the best performance, set the **vibratome slicing speed at 4 - 5 (~30 ± 4 mm/min), vibrating frequency at 85-87 Hz, and slicing amplitude at 4-6 (~1 ± 0.2 mm)**.
4. After brainstem sectioning, place the 200-300 µm sequentially collected slices in a commercially available slice chamber to equilibrate for 1 h at room temperature in ACSF, continuously bubbled with a mixture of 95% O₂/5% CO₂ (pH 7.2-7.4, osmolarity 300-310 mOsm/L). In these conditions, slices remain viable up to 5-6 h.

7. Electrophysiology: patch clamp procedure

1. Transfer a brainstem slice to the recording chamber with continuous perfusion of carboxygenated ACSF $\sim 1.5 \pm 0.5$ mL/min.
2. Pull patch pipettes with a micropipette puller of tip diameter 1-2 μm and resistance in the range of 3-6 M Ω .
 1. Fill pipettes with a K-Gluconate-based internal solution (for current-clamp recording).
3. To test the neuronal properties across the different tonotopic regions within a slice, locate neurons at either end of the slice plane and approach with the recording electrode.
4. Maintain positive air pressure at the pipette tip while approaching a neuron.
5. Move towards the soma until an indentation is visualized on the neuron. Perform the next two steps quickly.
6. Make a gigaohm (1 G Ω) seal by releasing positive air pressure.
7. Keep the amplifier setting in voltage-clamp mode and correct the pipette offset as zero pA. Run a seal test (10 mV test pulse at 100 Hz). Apply negative air-pressure to rupture a small patch of the neuronal membrane.
8. To test the active intrinsic properties of auditory neurons, apply hyperpolarizing and depolarizing somatic current injections.

NOTE: Examples of this procedure can be visualized in **Supplementary Video S1, S2**. Details of this procedure are provided in the video legends.

Representative Results

All brainstem slices shown here were acquired from brainstem tissue ($\sim 200\text{-}300$ μm) and imaged using a 5x objective and differential interference contrast (DIC) optics. The camera was mounted on the dissecting microscope and connected to a computer with image acquisition software (see **Table of Materials**). Satellite inset for these figures (right panels) were imaged using a 60x magnification water immersion objective. Care was taken to ensure that all areas of the brainstem slice were equally magnified while obtaining digital images. Photographs were taken at optimal brightness and focus. The digital images of brainstem slices were stitched in a planar fashion based on overlapping area and imported to a desktop computer for further adjustments of brightness, contrast, and grayscale. The basic microcircuits of the chicken auditory brainstem were identified according to previous work^{1,2,5,13}. Under the microscope (5x objective), auditory nuclei were identified as the area adjacent to the heavily myelinated nerve fibers coursing around each nucleus both ipsilaterally and contralaterally along the dorsal regions of the slice.

Figure 1 shows the traditional coronal sections of brainstem tissue (200-300 μm) from an E21 chicken embryo. The four coronal slices shown here represent the relative iso-frequency regions of the auditory brainstem nuclei, from the lowest-CF auditory region (**Figure 1A**, caudo-lateral) progressing to the highest-CF auditory region (**Figure 1D**, rostral-medial). For all four coronal slices in **Figure 1A-D**, magnified regions of labeled NM and NL are shown in the middle column and magnified (60x objective) on the right side of the figure panel (a and b, respectively, in satellite insets). The arrow in **Figure 1A,B** shows the input of auditory nerve fibers, and the arrowhead shows bifurcation of NM axons on

the left of the slice. **Figure 1C** shows another avian cochlear nucleus structure known as nucleus angularis (NA, arrow on left and arrowhead on right). The two most rostral coronal slices show the superior olivary nucleus (SON) located along the ventral-lateral region of the coronal slice (**Figure 1C,D**, white dashed circles).

Figure 2 shows sagittal sections of brainstem tissue (200-300 μm) from a E21 chicken embryo. For all three sagittal slices (**Figure 2A-C**), magnified regions of labeled NM and NL are shown in the middle column and magnified (60x objective) on the right side of the figure panel (a and b, respectively in satellite images). NM and NL were identified where the auditory nerve fibers (**Figure 2A**, middle arrow) entered the cluster of neurons observed at higher magnification (**Figure 2A**, middle, small, white dashed circles and arrowheads) and highlights the starting point of the auditory region (**Figure 2A**, left, large, white dashed circle and arrowhead). SON was identified in the rostro-lateral region of the most lateral slice (**Figure 2A**, small, white, dashed circle). **Figure 2B** shows extended tonotopic regions that contain both relatively low- and high-CF auditory regions from NM and NL along the rostral-caudal axis (white outlined regions, see also satellite inset). **Figure 2C** shows the ipsilateral and contralateral axonal tufts in the most medial slice and the endpoint of the auditory region (left and middle arrows). The orientation of the slices shown here contrast with the traditional orientation of slices as seen in **Figure 1** (i.e., coronal). This was performed to display the orientation that best accommodates the approach of a glass pipette required for electrophysiological recordings.

To confirm that a large region of the tonotopic axis was represented in **Figure 2B**, current-clamp electrophysiology recordings were performed from NM neurons. **Figure 3**

shows functional similarities and differences of mature (E21) NM neurons recorded from a coronal slice (**Figure 3A,B**) and a sagittal slice (**Figure 3C,D**, **Supplementary Video S1, S2**). Two NM neurons were selected from the medial and lateral ends of a coronal slice (similar to the slice shown in **Figure 1B**), and two NM neurons were selected from the rostral and caudal ends of NM in a sagittal slice (as in the slice shown in **Figure 2B**). **Figure 3A,B** shows similar electrophysiological response properties to somatic current injections (-100 pA to $+200$ pA, $+10$ pA increments, 100 ms duration). The firing pattern of these two NM neurons exhibits subtle differences in this slice plane, indicating relative iso-frequency lamina for mid-frequency NM neurons. **Figure 3C,D** show that the firing patterns have substantive differences across the rostral-caudal axis, indicating a relatively higher tonotopic gradient from a low frequency NM neuron (**Figure 3C**) to a high-frequency NM neuron (**Figure 3D**). Both neurons presented with their stereotypical firing patterns as previously reported^{14,15}.

Figure 4 shows horizontal sections of brainstem tissue (200-300 μm) of an E21 chicken embryo. For both horizontal slices (**Figure 4A,B**), magnified regions of labeled NM and NL are shown in the middle column and magnified (60x objective) on the right side of the figure panel (a and b, respectively, in satellite insets). In the horizontal slices, NM and NL were identified toward the midline and neurons were spread along the lateral-medial axis (**Figure 4A,B**, middle, white, dashed outline regions). The magnified images show the large extent of the tonotopic gradient. Low-frequency neurons are in the caudo-lateral regions and high-frequency neurons are in the rostral-medial areas (**Figure 4A,B**, right, satellites). The fibers running through the midline along the rostral-caudal axis show the contralateral connections of the auditory nuclei, but the organization of these fibers is not in a simple plane.

However, acute angular slices from a horizontal/transverse section can follow these axonal fibers towards the sagittal plane. Slices of 200-300 μM thick brainstem tissue at an acute angle (45°) from a horizontal plane are shown in **Figure 5**. Auditory brainstem nuclei can be seen across a large diagonal spread starting from the most lateral slice and ending at the most medial slice (**Figure 5A-C**, labeled middle panels, white outlined area). Moreover, the angular orientation of NM and NL regions can also be visualized in

successive asymmetrical slices (**Figure 5A-C**, labeled middle panels, white, dashed outlined area). Magnified images (60x objective) show the tonotopic axis of the auditory nuclei as it courses along the rostral-medial to caudo-lateral axis (**Figure 5A-C**, right, satellite inset). The orientation of slices in **Figure 5** is similar to that in **Figure 2**. They contrast the traditional presentation of images but are more suitable for electrophysiological experiments.

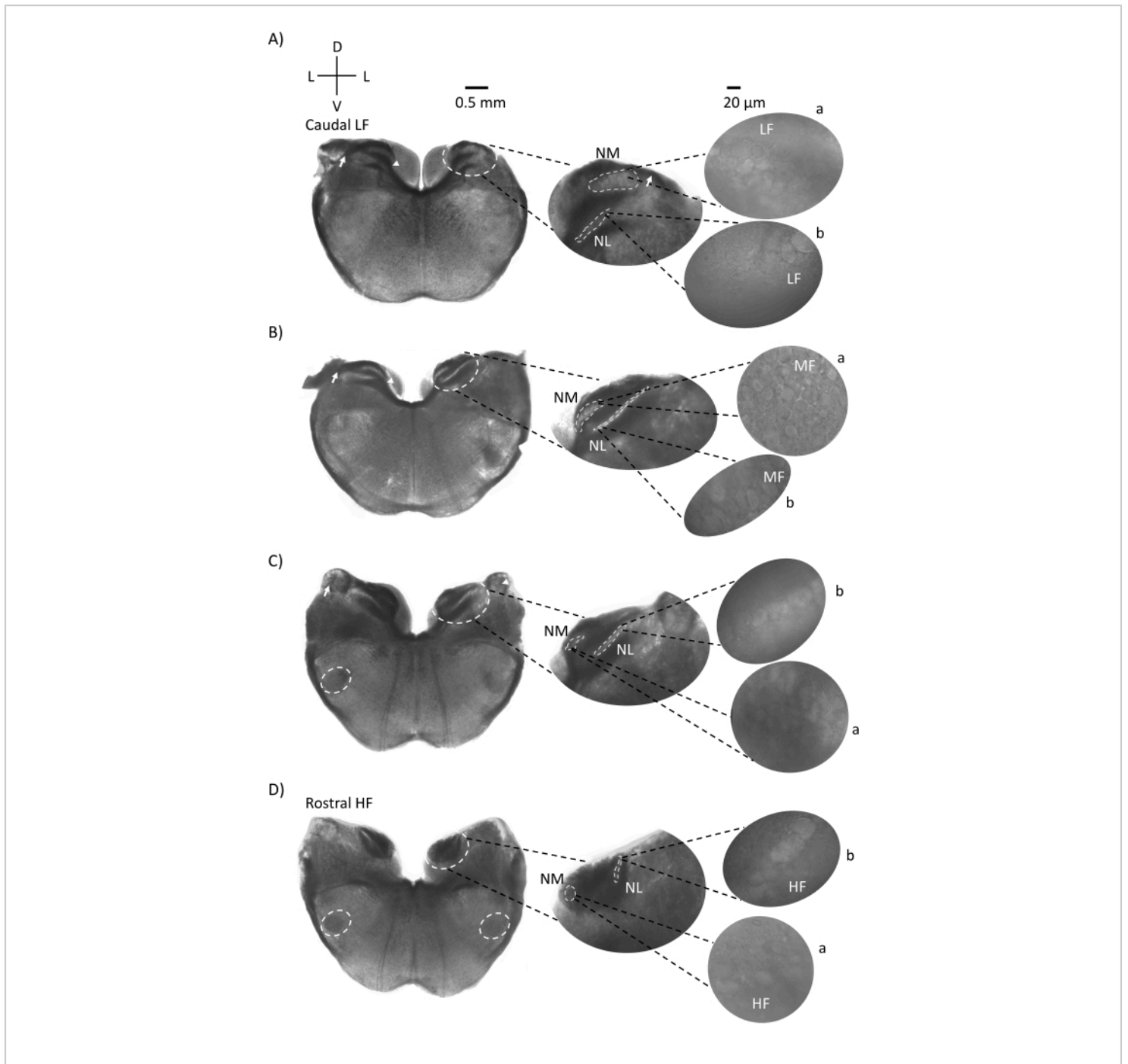


Figure 1: Representative coronal serial sections of the brainstem. (A-D) Left: slices from caudal to rostral axis, the auditory nuclei and connecting fibers marked with a white dashed circle. The middle insert is a larger view of the auditory region, where nuclei are shown within white dashed circles **a**: NM and **b**: NL. Arrows show auditory nerve afferent fibers, and arrowhead shows NM axon bifurcation in **A,B**. Arrow shows NA in **C**. Lateral white dashed circle shows SON in **C,D**. Right: satellite insert shows these nuclei at 60x objective: **a**: NM and **b**: NL. Abbreviations: NM = nucleus magnocellularis; NL = nucleus laminaris; NA = nucleus angularis; SON = superior olivary nucleus; LF = relatively low-frequency neurons; MF

= medium-frequency neurons; HF = high-frequency neurons; D = dorsal; L = lateral; V = ventral. [Please click here to view a larger version of this figure.](#)

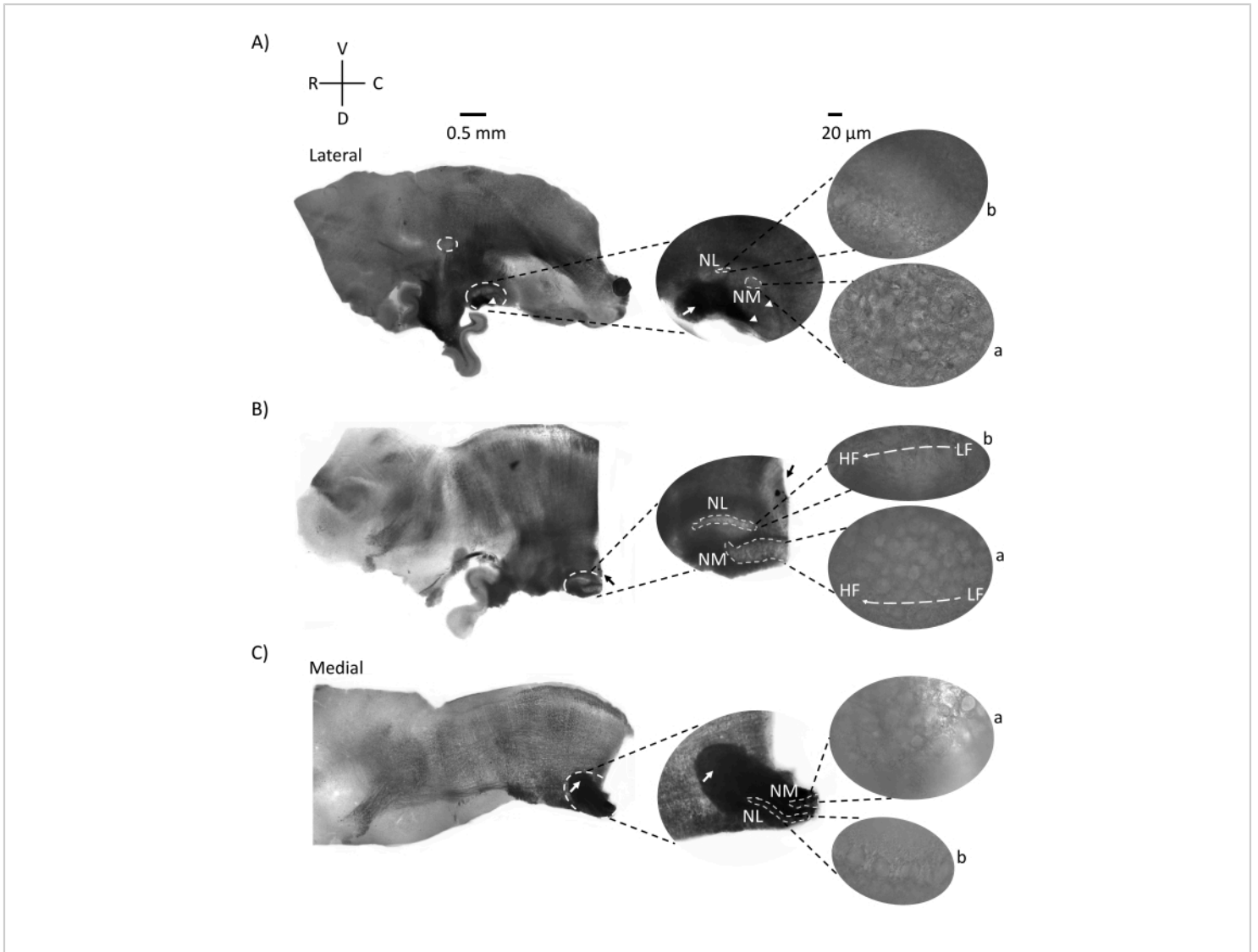


Figure 2: Representative sagittal serial sections of the brainstem. (A-C) Left: slices from lateral to medial axis with the auditory nuclei labeled in a white dashed circle. The middle insert shows the same auditory nuclei region in larger view, marked within white dashed circles. **(A)** White dashed circle in the center of slice highlights the SON; arrow showing auditory nerve fibers and arrowhead showing NA. A dark black spot at right-side tip of slice is an imaging artifact. Regions of the cerebellum can be seen dorsal to the auditory region in both slices **A** and **B** in left panel. **(B)** A sagittal slice whose orientation was changed to the coronal plane (during slicing). The auditory region was identified with blue dye (black arrow) and again sliced in the sagittal plane. **(A-C)** Middle insert NM and NL region marked under dashed white lines. Right: satellite view shows **a**: NM and **b**: NL observed in 60x objective magnification. LF and HF tonotopic gradient in auditory nuclei is shown along rostro-caudal axis. Arrows pointing to the dark area in **(C)** show heavily myelinated NM fibers running across the midline through the medial axis. The fibers connect either side of auditory nuclei. Abbreviations: NM = nucleus magnocellularis; NL = nucleus laminaris; NA = nucleus angularis; SON = superior olivary nucleus; LF = relatively low-

frequency neurons; HF = high-frequency neurons; D = dorsal; V = ventral; R = rostral; C = caudal. [Please click here to view a larger version of this figure.](#)

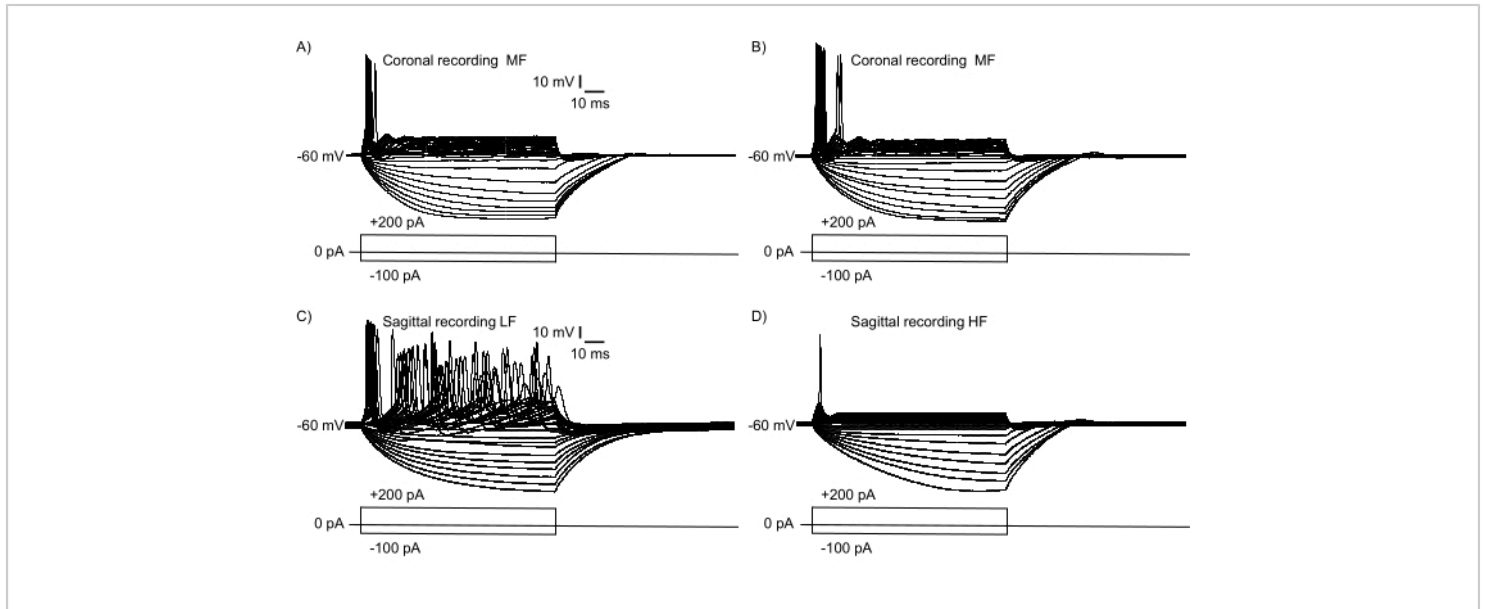


Figure 3: Electrophysiological recordings of neuronal response to somatic current injections (-100 pA to +200 pA, +10 pA increments, 100 ms duration) in current clamp mode. Neurons were selected for recordings in the same slice but at extreme opposite regions of NM. **(A,B)** Representative neuronal responses in a single coronal slice indicating relative iso-frequency properties with subtle differences. Response properties represent two different MF neurons recorded from the most medial **(A)** and lateral **(B)** regions of NM in a coronal slice. **(C,D)** Representative neuronal recordings from a single sagittal slice. The recordings show a relatively LF NM response **(C)** and a HF NM response **(D)**, highlighting the substantive differences in tonotopic gradient along within a single sagittal section. Abbreviations: NM = nucleus magnocellularis; LF = relatively low-frequency neurons; MF = mid-frequency neurons; HF = high-frequency neurons. [Please click here to view a larger version of this figure.](#)

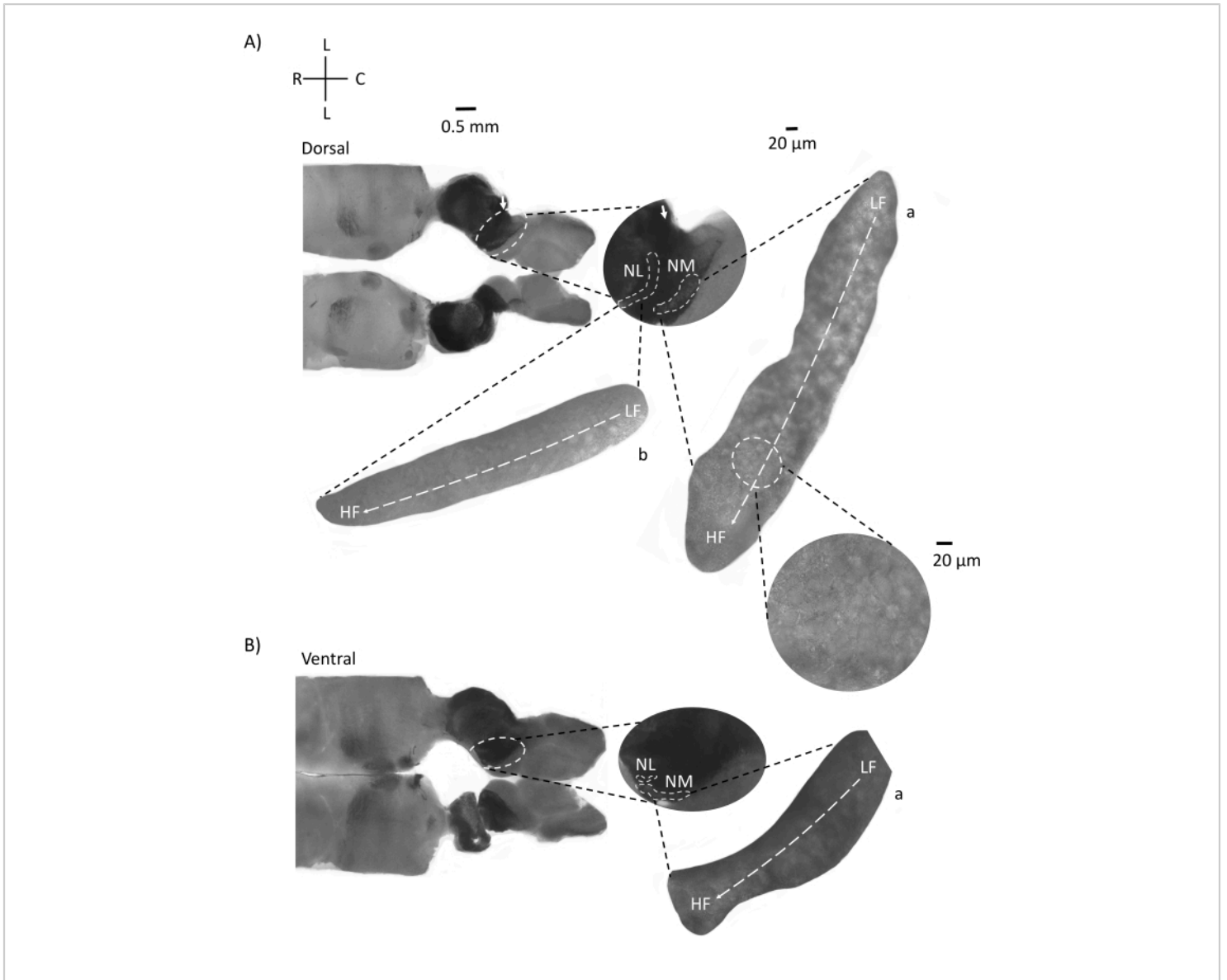


Figure 4: Representative horizontal serial sections of the brainstem. (A,B) Left: slices along the dorsal to ventral axis, auditory nuclei are marked with white dashed circles. The 8th cranial nerve afferent fibers connect auditory nuclei marked with arrow. The middle insert is a larger view of auditory nuclei region with auditory nuclei marked under white dashed lines NM and NL regions are shown. A clear topological movement of auditory nuclei can be seen in **A,B**. **(A,B)** Right: large satellite view showing **a**: NM and **b**: NL. Right insert shows auditory nuclei observed in 60x objective magnification and the curved topological axis from LF to HF along a caudo-lateral to rostral-medial axis. Abbreviations: NM = nucleus magnocellularis; NL = nucleus laminaris; LF = relatively low-frequency neurons; HF = high-frequency neurons; L = lateral; R = rostral; C = caudal. [Please click here to view a larger version of this figure.](#)

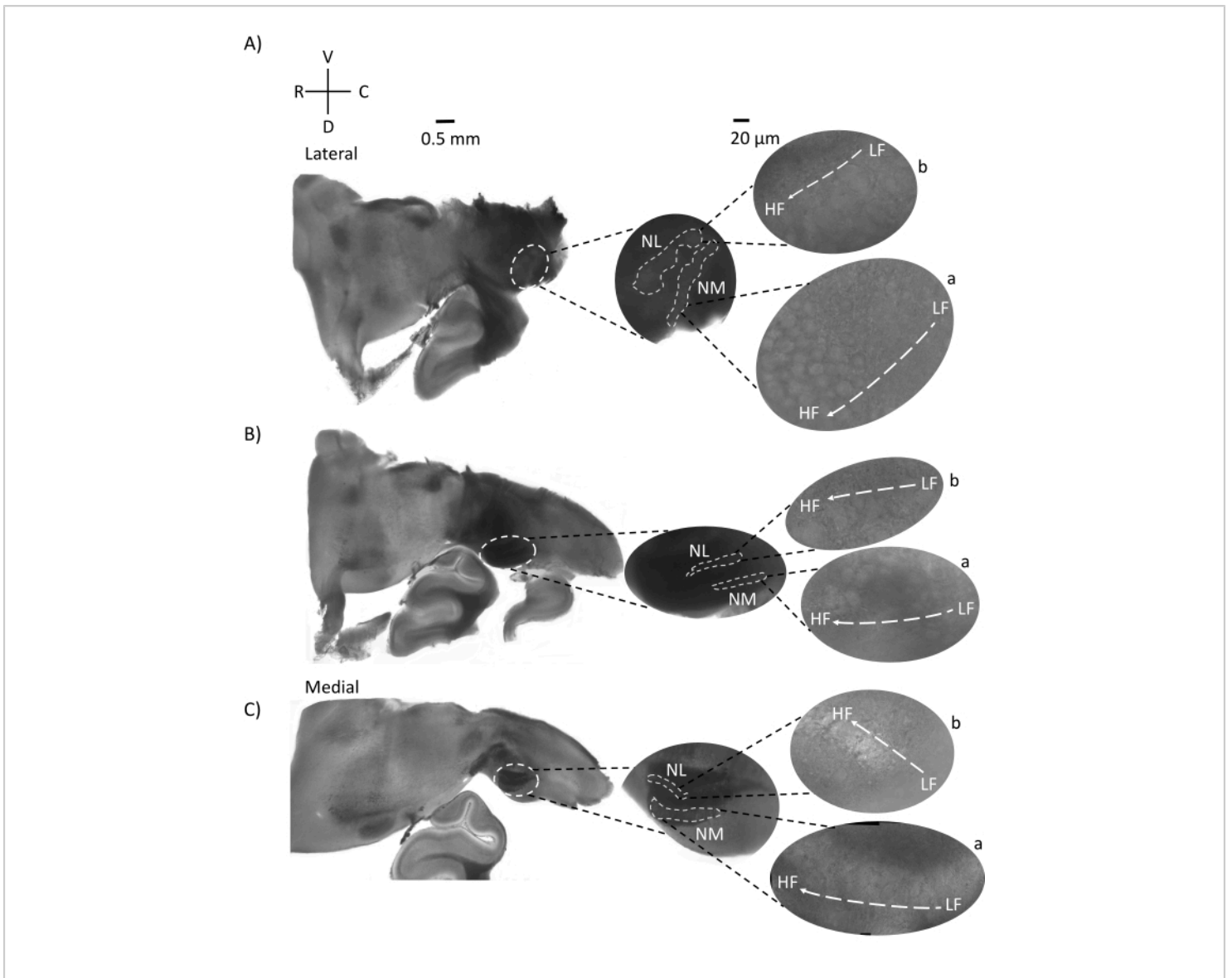


Figure 5: Representative horizontal/transverse acute angular (45°) serial sections. (A-C) Left: serial sections of the brainstem, auditory nuclei marked in white dashed circle. The middle insert is a larger view of the auditory region. **(A)** Middle insert shows the largest spread of NM and NL neurons in these slices. **(B,C)** Middle insert: auditory nuclei marked in white dashed lines show gradual topological change when compared to **(A-C)**. Right: satellite insert showing auditory nuclei **a**: NM and **b**: NL in 60x objective magnification. The tonotopic axis from LF to HF regions in NM and NL rotates angularly from lateral to medial slices. Abbreviations: NM = nucleus magnocellularis; NL = nucleus laminaris; LF = relatively low-frequency neurons; HF = high-frequency neurons; V = ventral; R = rostral; D = dorsal; C = caudal. [Please click here to view a larger version of this figure.](#)

Supplementary Video S1: Hyperpolarizing and depolarizing somatic current injections. Response properties from a low-frequency and high-frequency neuron to 100 ms somatic current injections in current clamp mode.

Neurons were selected from the same sagittal brainstem slice. Injections range from -100 to +200 pA in steps of +10 pA increments, 100 ms time duration. Action potentials are seen in response to sufficient depolarizing current steps. The video corresponds to the final traces shown in **Figure 3C**. [Please click here to download this File.](#)

Supplementary Video S2: Hyperpolarizing and depolarizing somatic current injections. Similar to **Supplementary Video S1**, this video shows response properties from a low-frequency and high-frequency neuron to 100 ms somatic current injections in current clamp mode. Neurons were selected from the same sagittal brainstem slice. Injections range from -100 to +200 pA in steps of +10 pA increments, 100 ms time duration. Action potentials are seen in response to sufficient depolarizing current steps. The video corresponds to the final traces shown in **Figure 3D**. [Please click here to download this File.](#)

Discussion

Coronal sections of chicken embryonic brainstem tissue have allowed the study of relative individual iso-frequency lamina for decades^{1,2,5}. However, the tonotopic (i.e., frequency) organization of the chicken auditory brainstem is topologically convoluted and may be more accessible in other anatomical axes depending on the specific research question. Although sufficient to investigate anatomical and physiological questions pertaining to individual iso-frequency regions, the study of tonotopic variations and its development across larger auditory brainstem areas are somewhat limited by coronal sections. To overcome this limitation, this protocol describes approaches in the sagittal, horizontal, and horizontal/transverse planes to provide additional examples of auditory brainstem tissue that exhibit maximum tonotopic properties and gradients in an individual brainstem section.

Sagittal sections of auditory brainstem regions show that different tonotopic areas are distributed across a larger region within the slice compared to coronal sections (sagittal auditory area = ~300-600 μm , coronal auditory area = ~200-350 μm). For example, NM and NL regions were visualized over a larger area along the rostro-caudal axis in sagittal sections (e.g., **Figure 2B**), and the functional tonotopic gradient that runs along this anatomical axis was largely contained within a single sagittal slice. This was further confirmed with current-clamp recordings of intrinsic neuronal differences that vary along the rostral-caudal gradient as previously reported^{14,15} (e.g., **Figure 3C,D**). Future experiments that highlight anatomical and immunohistochemical properties along the tonotopic axis could further investigate known gradients of auditory properties within a single sagittal slice plane. These include, but are not limited to, MAP2 staining and potassium channel expression patterns, which are known gradients of dendritic architecture and intrinsic properties of NM and NL that have been previously shown in successive coronal sections¹⁶.

Horizontal sections of auditory brainstem regions show that the NM and NL are located toward the midline. A portion of auditory axonal fibers run diagonally or perpendicular to the horizontal plane (**Figure 4**). These fibers can be followed by making an acute angular slice 45° to the sagittal plane. The resulting horizontal/transverse slices were larger than the sagittal or horizontal slices, and long axonal fibers coursed through the rostro-caudal axis for both ipsilateral and contralateral sides. Both NM and NL can be visualized in a larger diagonal region (~400-700 μm) such that contralateral connections can be visualized along a lateral-medial axis. Additionally, the horizontal/transverse slice plane also shows how the auditory regions and the resulting tonotopic gradient make an angular turn (**Figure 5**). Angular exposure of

contralateral connections in a larger area makes these slices more suitable for electrophysiological stimulation and microcircuitry studies than traditional coronal slices.

Additional advantages

The formation of auditory microcircuits requires spatiotemporal coordination of cues that promote neuronal survival, synaptogenesis, axonal differentiation, dendritic architecture, and maturation. Thus, an alternative brainstem sections of the chicken embryo auditory microcircuit can be used for the following research topics: morphological organization of neurons in topographically different dimensions; organizing and mapping the connectomes of all auditory and vestibular nuclei; identification and characterization of the activity patterns of circuit constituents in iso-frequency and tonotopic planes; the topographical organization of excitatory versus inhibitory microcircuits and relations to specialized neuron populations (nuclei); spatial location of auditory nuclei neurons and its predictive CF¹⁷; systematic targeting of specific tonotopic neuronal types; tracking progenitor cells and their development into conserved nuclei; genetic lineage of cells to the evolution of neuronal circuits¹⁸; comparative brainstem anatomy between species; investigation of vestibular circuits like Deiter's vestibular complex (DC)¹⁹; and synchrony and cross talk between vestibular nuclei.

A multifaceted approach using different slice planes may help answer fundamental questions about unknown anatomical and biophysical properties of brainstem microcircuits. A good example is the relationship between major auditory nuclei (NM, NA, NL, and SON) and the vestibular nuclei, including the dorsal nucleus of the lateral lemniscus (LLDp), the semilunar nucleus (SLu)²⁰, and the tangential nucleus (TN)³.

However, this protocol and these slice-based studies do have some limitations.

Precautions and limitations

Depending on the institution performing the experiments, ethical guidelines and the handling of chicken embryos may differ. While the National Institutes of Health Guidelines for the Care and Use of Laboratory Animals permits rapid decapitation, there are alternative methods for chicken embryo euthanasia²¹. Early developing chicken embryo brainstem tissue is soft, and delicate compared to older embryos. It has several connections and blood vessels on the surface that need extra caution when removing them. Tissue should be kept in ice-cold dACSF and perfused with 95% O₂/5% CO₂ to increase the viability.

The sagittal slicing method is only useful for ipsilateral tonotopy. This slicing method provides larger slices than coronal slices, the handling of which could be precarious. However, one can trim the slices using cross needle methods described in detail elsewhere²². Using 4% LMP agarose block embedded brainstem can save delicate structures in slices, but care must be taken not to pour excessively hot agarose. Setting it quickly by placing the agarose-blocked brainstem in a chilled environment for ~1 min makes slices more viable for electrophysiological recordings.

Application of superglue in excess amounts can be toxic. It must be applied minimally, and surplus amounts should be washed immediately by changing out the dACSF. For acute angular (45°) slices, cutting the angle of the agarose block is critical; one can use a mirror to see the front angle while cutting the agarose block with a sharp blade. Commercially available blades might have a wax coating which should be wiped off with alcohol and dried before use. Optimization is required for the vibratome cutting speed and frequency as

axonal fiber tufts are harder than cortical or matrix tissue. Keeping a high amplitude and using chilled dissection solution may prevent tissue damage.

All solutions should be prepared fresh, and Ca^{2+} and Mg^{2+} should be added to the ACSF after bubbling 95% O_2 /5% CO_2 . Otherwise, there may be precipitation of Ca^{2+} . A paintbrush should be used to handle the slices gently within the vibratome. Keep the total slicing time under 15 min if possible. A glass Pasteur pipette can be used to maneuver brainstem slices.

Do not use detergent or corrosive washing agents for glassware and equipment that contact the slices used in electrophysiology. The images taken represent the appearance of 200-300 μM thick tissue under differential interference contrast (DIC) optics. The visual quality will be poorer than immunohistochemistry or electron microscopy, but it accurately reflects what an experimenter will see when performing electrophysiological recordings.

Studies pertaining to the early development of microcircuits along an alternative anatomical axis, whether they are dorsal-ventral, rostral-caudal, or ipsilateral-contralateral, are limited in the chicken auditory brainstem. One reason for this is because the role of transcriptional codes and regulation of tonotopic development in the brainstem is still not fully understood. Functional phenomena such as top-down modulation and spontaneous activity are often lost when observing activity *in vitro*. However, *in vivo* research is complemented by specific and direct single neuron recordings only possible in these slice conditions. The refinement of obtaining brainstem tissue along different orientations could provide insightful information about the

development and complexity of tonotopic gradients in the chicken auditory brainstem microcircuitry.

Disclosures

All authors declare that the research was conducted without any commercial or financial interest and that they do not have any conflicts of interest.

Acknowledgments

This work is supported by the NIH/NIDCD R01 DC017167 grant. We thank Kristine McLellan for providing editorial comments on an earlier version of the manuscript.

References

1. Rubel, E. W., Parks, T. N. Organization and development of brain stem auditory nuclei of the chicken: tonotopic organization of n. magnocellularis and n. laminaris. *Journal of Comparative Neurology*. **164** (4), 411-433 (1975).
2. Rubel, E. W. et al. Organization and development of brain stem auditory nuclei of the chicken: ontogeny of n. magnocellularis and n. laminaris. *Journal of Comparative Neurology*. **166** (4), 469-489 (1976).
3. Shao, M. et al. Spontaneous synaptic activity in chick vestibular nucleus neurons during the perinatal period. *Neuroscience*. **127** (1), 81-90 (2004).
4. Fukui, I., Ohmori, H. Tonotopic gradients of membrane and synaptic properties for neurons of the chicken nucleus magnocellularis. *Journal of Neuroscience*. **24** (34), 7514-7523 (2004).
5. Sanchez J. T., Seidl A. H., Rubel E. W., Barria A. Preparation and culture of chicken auditory brainstem

- slices. *Journal of Visualized Experiments*. (49), 2527 (2011).
6. Sanchez, J. T., Lu, Y. Glutamate signaling in the auditory brainstem. In: Fay, R. R., Popper, A.N., Cramer, K., Coffin, A. (Eds.), New York, NY: Springer. *Auditory Development and Plasticity: Springer Handbook of Auditory Research*. **64** (4), 75-108. (2017).
 7. Parks, T. N. Morphology of axosomatic endings in an avian cochlear nucleus: nucleus magnocellularis of the chicken. *Journal of Comparative Neurology*. **203** (3), 425-440 (1981).
 8. Jhaveri, S., Morest, D. K. Sequential alterations of neuronal architecture in nucleus magnocellularis of the developing chicken: a Golgi study. *Neuroscience*. **7** (4), 837-853 (1982).
 9. Carr, C. E., Boudreau, R. E. Central projections of auditory nerve fibers in the barn owl. *Journal of Comparative Neurology*. **314** (2), 306-318 (1991).
 10. Köppl, C. Auditory nerve terminals in the cochlear nucleus magnocellularis: differences between low and high frequencies. *Journal of Comparative Neurology*. **339** (3), 438-446 (1994).
 11. Fukui, I. et al. Improvement of phase information at low sound frequency in nucleus magnocellularis of the chicken. *Journal of Neurophysiology*. **96** (2), 633-641 (2006).
 12. Wang, X. et al. Postsynaptic FMRP regulates synaptogenesis *in vivo* in the developing cochlear nucleus. *Journal of Neuroscience*. **38** (29), 6445-6460 (2018).
 13. Lu, T., Cohen, A. L., Sanchez, J. T. *In ovo* electroporation in the chicken auditory brainstem. *Journal of Visualized Experiments*. (124), e55628 (2017).
 14. Hong, H., Sanchez, J. T. Need for speed and precision: structural and functional specialization in the cochlear nucleus of the avian auditory system. *Journal of Experimental Neuroscience*. (12), 1-16 (2018).
 15. Hong, H. et al. Diverse intrinsic properties shape functional phenotype of low-frequency neurons in the auditory brainstem. *Frontiers in Cellular Neuroscience*. **12**, 1-24 (2018).
 16. Wang, X., Hong, H., Brown, D. H., Sanchez, J. T., Wang, Y. Distinct neural properties in the low-frequency region of the chicken cochlear nucleus magnocellularis. *eNeuro*. **4** (2), 1-26 (2017).
 17. Tabor, K. M. et al. Tonotopic organization of the superior olivary nucleus in the chicken auditory brainstem. *Journal of Comparative Neurology*. **520** (7), 1493-1508 (2012).
 18. Lipovsek, M., Wingate, R. J. Conserved and divergent development of brainstem vestibular and auditory nuclei. *Elife*. **7**, e40232 (2018).
 19. Passetto, M. F. et al. Morphometric analysis of the AMPA-type neurons in the Deiter's vestibular complex of the chick brain. *Journal of Chemical Neuroanatomy*. **35** (4), 334-345 (2008).
 20. Curry, R. J., Lu, Y. Intrinsic properties of avian interaural level difference sound localizing neurons. *Brain Research*. **1752**, 147258 (2021).
 21. Aleksandrowicz, E. and Herr, I. Ethical euthanasia and short-term anesthesia of the chick embryo. *ALTEX - Alternatives to Animal Experimentation*. **32** (2), 143-147 (2015).

22. Palkovits, M. Isolated removal of hypothalamic or other brain nuclei of the rat. *Brain Research*. **14** (59), 449-450 (1973).